


Geometric Origin of the Tennis Racket Effect

P. Mardešić^{1,*}, G. J. Gutierrez Guillen², L. Van Damme³, and D. Sugny^{3,†}

¹*Institut de Mathématiques de Bourgogne—UMR 5584 CNRS, Université de Bourgogne-Franche Comté, 9 avenue Alain Savary, BP 47870, 21078 Dijon, France*

²*Instituto de Matemáticas, Universidad Nacional Autónoma de México (UNAM), Area de la Investigación Científica, Circuito exterior, Ciudad Universitaria, 04510 Ciudad de México, México*

³*Laboratoire Interdisciplinaire Carnot de Bourgogne (ICB), UMR 6303 CNRS-Université de Bourgogne-Franche Comté, 9 avenue Alain Savary, BP 47870, 21078 Dijon Cedex, France*

 (Received 23 March 2020; revised 8 June 2020; accepted 14 July 2020; published 6 August 2020)

The tennis racket effect is a geometric phenomenon which occurs in a free rotation of a three-dimensional rigid body. In a complex phase space, we show that this effect originates from a pole of a Riemann surface and can be viewed as a result of the Picard-Lefschetz formula. We prove that a perfect twist of the racket is achieved in the limit of an ideal asymmetric object. We give upper and lower bounds to the twist defect for any rigid body, which reveals the robustness of the effect. A similar approach describes the Dzhanibekov effect in which a wing nut, spinning around its central axis, suddenly makes a half-turn flip around a perpendicular axis and the monster flip, an almost impossible skateboard trick.

DOI: [10.1103/PhysRevLett.125.064301](https://doi.org/10.1103/PhysRevLett.125.064301)

Consider an experiment that every tennis player has already made. The tennis racket is held by the handle and thrown in the air so that the handle makes a full turn before catching it. Assume that the two faces of the head can be distinguished. It is then observed, once the racket is caught, that the two faces have been exchanged. The racket did not perform a simple rotation around its axis, but also an extra half-turn. This twist is called the tennis racket effect (TRE). An intuitive understanding of TRE is given in Ref. [1]. It is also known as the Dzhanibekov's effect (DE), named after the Russian cosmonaut who made a similar experiment in 1985 with a wing nut in zero gravity [2,3]. The wing nut spins rapidly around its central axis and flips suddenly after many rotations around a perpendicular axis [3]. The monster flip effect (MFE) is a freestyle skateboard trick. It consists in jumping with the skateboard and making it turn around its transverse axis with the wheels falling back to the ground. This trick is very difficult to execute since TRE predicts precisely the opposite, turning about this axis should produce a π flip and the wheels should end up in the air. The video in Ref. [4] shows that this trick can be made with success after several attempts.

We propose in this Letter to describe these phenomena. The results are established for a tennis racket and then extended to the two other systems. The motion is modeled as a free rotation of an asymmetric rigid body, which has three different moments of inertia along its three inertia axes [5]. The axes with the smallest and largest moments of inertia are stable, while the intermediate one is unstable. It is precisely this instability which is at the origin of TRE [6]. A more detailed description can be obtained from Euler's equations. The three-dimensional rotation is an example of

Hamiltonian integrable systems [7] in which the trajectories can be expressed analytically. The dynamics of the rigid body in the space-fixed frame are given by elliptic integrals of the first and third kinds, which lead to a very accurate description of TRE [6,8,9]. However, this analysis does not reveal its geometric character. A geometric point of view provides valuable physical insights, in particular with respect to the robustness of the corresponding physical phenomenon. Different geometric structures have been studied recently in the context of mechanical systems with a small number of degrees of freedom. Among others, we can mention the Berry phase [10], Hamiltonian monodromy [11–13], singular tori [14], and the Chern number [15], which found applications in classical and quantum physics. In this Letter, we show that the geometric origin of TRE is a pole of a Riemann surface defined in a complex phase space. This effect can be interpreted as the result of the Picard-Lefschetz formula which describes the possible deformation of an integration contour in a complex space after pushing it around a singular fiber [16,17]. The geometric character of DE and MFE can also be deduced from this approach and helps understanding in which conditions they can be realized. Note that similar complex methods have been used to describe Hamiltonian monodromy [18–20].

The position of the body-fixed frame (x, y, z) with respect to the space-fixed frame (X, Y, Z) defines the free rotation of a rigid body [2,5,7]. Three Euler angles (θ, ϕ, ψ) characterize the relative motion of the body-fixed frame. The angle θ is the angle between the axis z and the space-fixed axis Z . The rotation of the body about the axes Z and z is, respectively, described by the angles ϕ and ψ (see

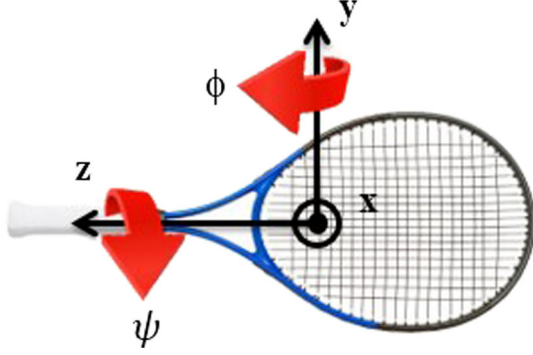


FIG. 1. A tennis racket with the three inertia axes (x, y, z) . The angles ϕ and ψ used to define TRE describe, respectively, the rotation of the body around the y and z axes. TRE is a phenomenon in which a full turn in ϕ direction produces an almost perfect half-turn in ψ direction.

Supplemental Material, Sec. II [21]). The moments of inertia I_x , I_y , and I_z are the elements of the diagonal inertia matrix in the body-fixed frame, with the convention $I_z < I_y < I_x$. As displayed in Fig. 1, a tennis racket is a standard example of an asymmetric rigid body in which the z axis is along the handle of the racket, y lies in the plane of the head of the racket, and x is orthogonal to the head (see Supplemental Material, Sec. I [21]). TRE consists in a 2π rotation of the body around the y axis. The precession of the handle is measured by the angle ϕ . TRE then manifests by a twist of the head about the z axis, i.e., by a variation $\Delta\psi = \pi$, along a trajectory such that $\Delta\phi = 2\pi$ [9].

Tennis racket effect.—TRE is a geometric phenomenon which does not depend on time. From Euler's equation, it can be described by the evolution of ψ with respect to ϕ (see Supplemental Material, Sec. II [21]):

$$\frac{d\psi}{d\phi} = \pm \frac{\sqrt{(a + b\cos^2\psi)(c + b\cos^2\psi)}}{1 - b\cos^2\psi}, \quad (1)$$

where we introduce the parameters $a = (I_y/I_z) - 1$, $b = 1 - (I_y/I_x)$, and $c = (2I_y H/J^2) - 1$, with the constraints $-b < c < a$, $a > 0$, and $0 < b < 1$. H and J denote, respectively, the rotational Hamiltonian and the angular momentum of the rigid body defined in Supplemental Material, Sec. II [5,21]. In the limit of a perfect asymmetric body, $I_z \ll I_y \ll I_x$, we deduce that $b \rightarrow 1$ and $a \rightarrow +\infty$. We consider only the positive values of $d\psi/d\phi$ defined in Eq. (1); the same analysis can be done for the negative sign. Equation (1) defines a two-dimensional reduced phase space with respect to ψ and $d\psi/d\phi$, as displayed in Fig. 2. Note the similarity of this phase space with the one of a planar pendulum, except that two consecutive unstable fixed points are separated by π instead of 2π . The separatrix for which $c = 0$ is the trajectory connecting these points [5]. We extend below the study to

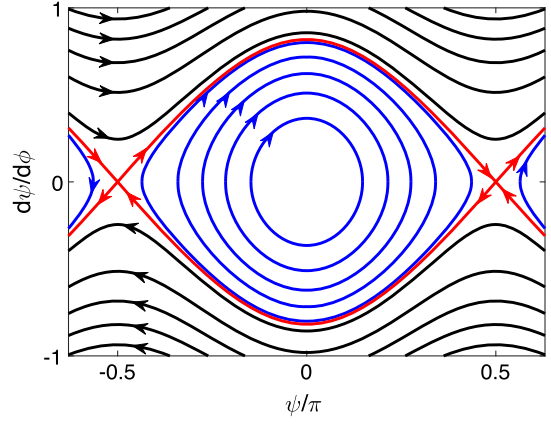


FIG. 2. Reduced phase space describing the dynamics of the rigid body in the space $(\psi, d\psi/d\phi)$. The black and blue (dark gray) lines depict, respectively, the rotating and oscillating trajectories of the angular momentum. The solid red line (light gray) represents the separatrix. The parameters a and b are set, respectively, to 12 and 0.05.

the complex domain and continue analytically all the functions.

TRE is associated with a trajectory for which $\Delta\psi \simeq \pi$ when $\Delta\phi = 2\pi$. We denote by ψ_0 and ψ_f the initial and final values of the angle ψ . To simplify the study of TRE, we consider a symmetric configuration for which $\psi_0 = -\pi/2 + \epsilon$ and $\psi_f = \pi/2 - \epsilon$. A perfect TRE is thus achieved in the limit $\epsilon \rightarrow 0$. Note that this symmetry hypothesis is not restrictive, as shown numerically in Supplemental Material, Sec. VI [21]. Using Eq. (1), we obtain that the variation of ϕ is given by

$$\Delta\phi = \int_{-\pi/2+\epsilon}^{\pi/2-\epsilon} \frac{1 - b\cos^2\psi}{\sqrt{(a + b\cos^2\psi)(c + b\cos^2\psi)}} d\psi. \quad (2)$$

For oscillating trajectories, the condition $c + b\cos^2\psi \geq 0$ leads to $\sin^2\epsilon \geq |c/b|$. From the parity of the integral and the change of variables $x = \cos^2\psi$, $\Delta\phi$ can be expressed as an incomplete elliptic integral, $\Delta\phi(\epsilon) = \int_{\sin^2\epsilon}^1 \omega$, with

$$\omega = \frac{1}{b} \frac{1 - bx}{\sqrt{x(x-\beta)(1-x)(x-\alpha)}} dx, \quad (3)$$

where $\alpha = -a/b$ and $\beta = -c/b$. As explained in Supplemental Material, Sec. III [21], we introduce a function M defined by $M(u_0) = [2 \ln(1 + \sqrt{2})]/[\sqrt{1 - u_0}] + 2 \ln(2)$ for $u_0 \in]0, 1[$, and $m = M(1/2) \simeq 3.879$. A precise description of TRE is given by Theorem 1, which is the main result of this study. Note that the statement is true slightly more generally for any value $u_0 \in]0, 1[$, by replacing everywhere m by $M(u_0)$. We put $u_0 = 1/2$ in Theorem 1 for simplicity.

Theorem 1.—For all c such that

$$|c| < b \exp(-2\pi\sqrt{ab} - m),$$

for ab large enough, the equation

$$\Delta\phi_{a,b,c}(\epsilon) = 2\pi$$

has a unique solution $\epsilon_S(a, b, c)$ which verifies

$$\arcsin\left[\sqrt{\left|\frac{c}{b}\right|}\right] < \epsilon_S < \arcsin\left[\exp\left(-\pi\sqrt{ab} - \frac{m}{2}\right)\right]. \quad (4)$$

This leads to

$$\lim_{ab \rightarrow +\infty} \epsilon_S(a, b, c) = 0.$$

Several questions about its existence, uniqueness, and robustness are raised by the observation of TRE; all find a rigorous answer in Theorem 1. A first fundamental comment concerns a perfect TRE which occurs only in the limit of a very asymmetric body. Such limits are common enough in physics to reveal specific phenomena. An example is given by the adiabatic evolution in mechanics [7] which is also based mathematically on an asymptotic analysis. The main statement of Theorem 1 describes the asymptotic behavior of the twist defect which approximately evolves as $\epsilon \simeq e^{-\sqrt{ab}\Delta\phi/2}$ for a sufficiently asymmetric body (with $ab \gg 1$). This exponential evolution is connected to the instability of the fixed points and to the presence of a pole in a complex phase space. The existence of a unique symmetric configuration realizing TRE follows from this asymptotic analysis. The corresponding trajectory is closer and closer to the separatrix for more asymmetric body (i.e., c goes to 0). Theorem 1 also establishes the robustness of TRE with respect to the shape of the body. Lower and upper bounds to the twist defect are given by Eq. (4) as a function of the different parameters.

These results have a geometric origin in the complex domain. We study the solution ϵ of $\Delta\phi_{a,b,c}(\epsilon) = 2\pi$, where $\Delta\phi = \Delta\phi_{a,b,c}$ is given by Eq. (2). The origin of TRE is revealed by a complexification of the problem in which $\Delta\phi$ can be interpreted as an Abelian integral over the Riemann surface of the form ω [17]. As displayed in Fig. 3, this surface has two sheets with four branch points in $x = 0, 1, \beta$, and α . Branch cuts are introduced to define a single-valued function. In the limit $c \rightarrow 0$, the two branch points $x = 0$ and $x = \beta$ coincide, leading to a pole whose integral is the logarithmic function. For large values of a , note that there is no confluence of the branch point $x = \alpha$ with $x = \beta$ or 0.

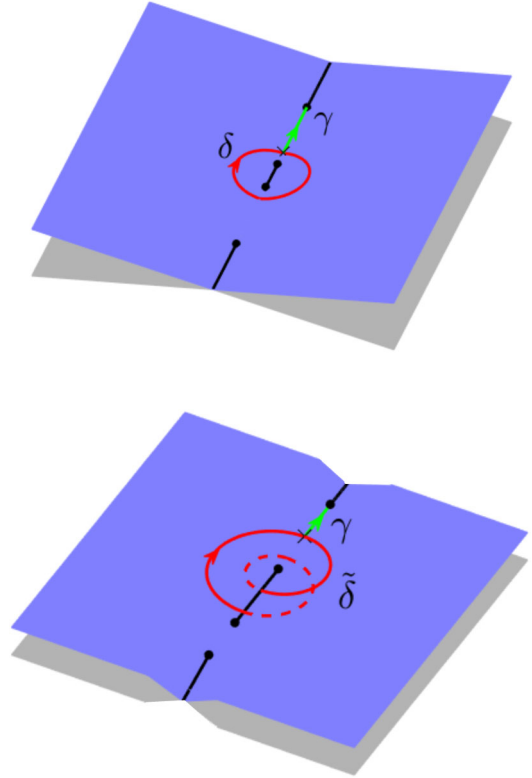


FIG. 3. Riemann surface of the form ω with the four branch points (black dots) in $x = \alpha, \beta, 0$, and 1 (from bottom to top). When $c \rightarrow 0$, the two points $x = \beta$ and $x = 0$ coincide and give birth to a pole. The top and bottom panels represent the cases where the TRE can or cannot be observed. The solid straight lines represent the branch cuts of the surface. The cycles δ and $\tilde{\delta}$ are depicted by solid red (dark gray) lines. The form ω is integrated along the path γ between the point u (black cross) and the ramification point $x = 1$ (green or light gray solid line).

Let F be the function defined by

$$F_{a,b,c}(u) = \int_u^1 \omega = \int_\gamma \omega,$$

where γ is the integration path with $0 < u < 1$. We have $\Delta\phi_{a,b,c}(\epsilon) = F_{a,b,c}(\sin^2 \epsilon)$. The multivalued character of $F_{a,b,c}$ is different for $u < |\beta|$ and $u > |\beta|$. In the case $|\beta| < u < 1$, we consider in the upper sheet of the Riemann surface the cycle δ passing by $x = u$ and encircling the two branch points β and 0 , as displayed in Fig. 3. By the Picard-Lefschetz formula [16,17], the integration contour γ is deformed to itself plus δ when the point $x = u$ performs a loop along δ . The integral $\int_\delta \omega$ adds to $F_{a,b,c}$, which reveals the multivalued character of $F_{a,b,c}$ as a complex function. A single-valued function can be obtained by adding a convenient multiple of $\ln u = -\int_u^1 (dx/x)$, the factor being given by $(1/2\pi i) \int_\delta \omega$. In the limit $c \rightarrow 0$, ω has a pole in $x = 0$ and this integral can be computed from a residue formula.

We present a heuristic proof of Theorem 1, while a rigorous demonstration is provided in Supplemental Material, Sec. III [21]. We consider a simplified version of the problem where only two branch points are accounted for. We have

$$\int_u^1 \frac{1}{\sqrt{x(x-\beta)}} dx = 2 \ln(\sqrt{x-\beta} + \sqrt{x}) \Big|_{x=u}^1.$$

Using the pole at infinity, we deduce that $(1/2\pi i) \int_{\delta} (dx/x) = 1$ and

$$\int_u^1 \left[\frac{1}{\sqrt{x(x-\beta)}} - \frac{1}{x} \right] dx = 2 \ln \left(\frac{1 + \sqrt{1-\beta}}{1 + \sqrt{1-\frac{\beta}{u}}} \right),$$

which is a well-defined and bounded function of u for $|\beta| < u < 1$. As shown in Supplemental Material, Sec. III [21], this argument can be generalized to $F_{a,b,c}$, which can be expressed as

$$F_{a,b,c}(u) = \frac{1}{\sqrt{ab}} h_{a,b,c}(u) - \frac{1}{\sqrt{ab}} \ln u, \quad (5)$$

where $h_{a,b,c}$ is an analytic and bounded function in $|\beta|, u_0$ with $0 < u_0 < 1$. The bound of $h_{a,b,c}$ is the function M introduced in Theorem 1. For ab large enough, the equation $F_{a,b,c}(u) = 2\pi$ has a unique solution which proves Theorem 1. In the second region in which $u < |\beta|$, the geometric situation is completely different, as can be seen in Fig. 3. The cycle $\tilde{\delta}$ encircles only the branch point $x = 0$ and no pole occurs when $c \rightarrow 0$. Turning twice around $x = 0$ to get a closed path, we obtain $\int_{\tilde{\delta}} \omega = 0$. This result stems from integrating the complex function $x \mapsto 1/\sqrt{x}$ along $\tilde{\delta}$. The function $F_{a,b,c}$ is bounded with no logarithmic divergence. No information is gained about the existence, the uniqueness, and the value of ϵ , i.e., the possibility to realize TRE.

Dzhanibekov effect.—A similar analysis can be used to describe DE [3]. As represented in Supplemental Material, Sec. I, the z - and x -inertia axes of this rigid body are, respectively, along the wings and orthogonal to the wings, while the y -inertia axis corresponds to the central axis of the rotation [21]. The video in Ref. [3] clearly shows that the motion of the wing nut is first guided by a screw which induces an almost perfect rotation around the central axis. In terms of Euler's angles, this leads to a very large angular velocity $\dot{\phi}$ and a speed $\dot{\psi}$ approximately equal to 0 (i.e., $d\psi/d\phi \simeq 0$). Since the device generating the rotation of the rigid body blocks the flip motion, the angle ψ is initially of the order of $\pm\pi/2$. We deduce that the initial point of the dynamics is very close to one of the unstable fixed points represented in Fig. 2, with a parameter $c \simeq 0$. Using Eq. (1), DE is described by

$$\Delta\phi = \int_{-\pi/2}^{\pi/2} \frac{1 - b\cos^2\psi}{\sqrt{(a + b\cos^2\psi)(c + b\cos^2\psi)}} d\psi,$$

with $c > 0$, where $\Delta\phi$ represents the angle increment before the flip of the system. We assume that the wing nut performs a perfect twist for which ψ goes from $-\pi/2$ to $\pi/2$. We show in Supplemental Material, Sec. IV [21], that

$$\Delta\phi = \frac{1}{\sqrt{ab}} [h_{a,b}(c) - \ln(c)], \quad (6)$$

where $h_{a,b}$ is a bounded function when $c \rightarrow 0$. In this limit, the logarithmic divergence of $\Delta\phi$ occurs with the confluence of the two branch points in $x = \beta$ and $x = 0$, which gives a pole as in TRE. Consequently, the speed $d\phi/d\psi$ increases tremendously in the neighborhood of this point. Note that the parameter c for DE plays the same role as ϵ for TRE, as can be seen in Eqs. (5) and (6). DE with many rotations around the intermediate axis can be observed for a sufficient small positive value of c . We stress that the number of turns does not need to be complete.

Monster flip.—This approach can be used for a skateboard where the z - and y -inertia axes are, respectively, orthogonal and parallel to the wheel axis, while the x axis is orthogonal to the board (see Supplemental Material, Sec. I [21]). MFE corresponds to a complete turn around the transverse axis together with a small variation of ψ . It can be realized in a neighborhood of the unstable point where $d\psi/d\phi = 0$ (i.e., $d\phi/d\psi = \infty$). We search for a solution ϵ close to zero of $\tilde{\Delta}\phi(\epsilon) = 2\pi$, where

$$\tilde{\Delta}\phi(\epsilon) = 2 \int_{\psi_i}^{\pi/2+\epsilon} \frac{1 - b\cos^2\psi}{\sqrt{a + b\cos^2\psi} \sqrt{c + b\cos^2\psi}} d\psi, \quad (7)$$

with $\psi_i = \pi/2$ and $\psi_i = \pi/2 + \arcsin[\sqrt{|\beta|}]$ for rotating and oscillating trajectories, respectively. As in TRE, we get $\tilde{\Delta}\phi(\epsilon) = \int_{\cos^2\psi_i}^{\sin^2\epsilon} \omega$, where ω is defined by Eq. (3). Introducing $\tilde{F}_{a,b,c}(u) = \int_{\cos^2\psi_i}^u \omega$, it can be shown in the region $|\beta| < u < 1$ that (see Supplemental Material, Sec. V [21])

$$\tilde{F}_{a,b,c}(u) = \frac{1}{\sqrt{ab}} \tilde{h}_{a,b,c}(u) + \frac{1}{\sqrt{ab}} \ln(u),$$

where $\tilde{h}_{a,b,c}$ is a bounded and single-valued function. Note the change of sign in front of the logarithmic term with respect to Eq. (5). The solution of $\tilde{\Delta}\phi_{a,b,c} = \tilde{F}_{a,b,c}(u)$ can be approximated as $\epsilon \simeq (\sqrt{|\beta|}/2) e^{\pi\sqrt{ab}}$. The accuracy of this approximation is shown numerically in Supplemental Material, Sec. VI [21]. For a body with $ab \geq 1$, MFE can be observed only in a neighborhood of the separatrix where $|\beta| \ll 1$. The rotation of the skateboard around its transverse

axis is constrained by the condition $\epsilon \geq \sqrt{|\beta|}$. This result quantifies the difficulty of performing MFE. For an angle ϵ of 30° , this leads for a standard skateboard to $c \simeq 10^{-3}$, while the maximum value of c is of the order of 10. Finally, as illustrated in Supplemental Material, Sec. V, MFE cannot be realized in the second region $u < |\beta|$ [21].

Conclusion.—TRE originates from a pole of a Riemann surface and a perfect twist of the head of the racket occurs in the limit of an ideal asymmetric body. Different properties such as the robustness of the effect have been derived from this geometric analysis. As a by-product, we have described DE and established why the MFE is so difficult to perform. This study paves the way for the analysis of other classical integrable systems and strongly suggests the importance of complex geometry beyond the cases studied in this Letter. An intriguing question is to transpose this effect to the quantum world. Different molecular systems could show traces of this effect [22,23]. Another field of application is the control of quantum systems by external electromagnetic fields [24] using, e.g., the analogy between Bloch and Euler equations [25].

This work was supported by the Ecole Universitaire de Recherche (EUR)-EIPHI Graduate School (Grant No. 17-EURE-0002).

*pavao.mardesic@u-bourgogne.fr

†dominique.sugny@u-bourgogne.fr

- [1] The Bizarre Behavior of Rotating Bodies, Explained, A video about TRE is available at, https://www.youtube.com/watch?v=1VPfZ_XzisU.
- [2] O. O'Reilly, *Intermediate Dynamics for Engineers: Newton-Euler and Lagrangian Mechanics* (Cambridge University Press, Cambridge, England, 2020).
- [3] See the video at <https://www.youtube.com/watch?v=1x5UiwEEvpQ>; see also H. Murakami, O. Rios, and T. J. Impelluso, *J. Appl. Mech.* **83**, 111006 (2016); P. M. Trivailo and H. Kojima, *Trans. JSASS Tech. Jpn.* **17**, 72 (2019).
- [4] See <https://www.youtube.com/watch?v=vkMmbWYnBHg>; <https://www.youtube.com/watch?v=yFRPhi0jhGc>.
- [5] H. Goldstein, *Classical Mechanics* (Addison-Wesley, Reading, MA, 1950).
- [6] R. H. Cushman and L. Bates, *Global Aspects of Classical Integrable Systems* (Birkhauser, Basel, 1997).
- [7] V. I. Arnold, *Mathematical Methods of Classical Mechanics* (Springer-Verlag, New York, 1989).
- [8] M. S. Ashbaugh, C. C. Chicone, and R. H. Cushman, The twisting tennis racket, *J. Dyn. Differ. Equ.* **3**, 67 (1991).
- [9] L. Van Damme, P. Mardešić, and D. Sugny, The tennis racket effect in a three-dimensional rigid body, *Physica (Amsterdam)* **338D**, 17 (2017).
- [10] A. Bohm, A. Mostafazadeh, H. Koizumi, Q. Niu, and J. Zwanziger, *The Geometric Phase in Quantum Systems* (Springer, Berlin, 2003).
- [11] K. Efstathiou, *Metamorphoses of Hamiltonian Systems with Symmetry*, Lecture Notes in Mathematics Vol. 1864 (Springer-Verlag, Heidelberg, 2004).
- [12] N. J. Fitch, C. A. Weidner, L. P. Parazzoli, H. R. Dullin, and H. J. Lewandowski, Experimental Demonstration of Classical Hamiltonian Monodromy in the 1:1:2 Resonant Elastic Pendulum, *Phys. Rev. Lett.* **103**, 034301 (2009).
- [13] R. H. Cushman, H. R. Dullin, A. Giacobbe, D. D. Holm, M. Joyeux, P. Lynch, D. A. Sadovskii, and B. I. Zhilinskii, CO₂ Molecule as a Quantum Realization of the 1:1:2 Resonant Swing-Spring with Monodromy, *Phys. Rev. Lett.* **93**, 024302 (2004).
- [14] D. Sugny, A. Picozzi, S. Lagrange, and H. R. Jauslin, Role of Singular Tori in the Dynamics of Spatiotemporal Nonlinear Wave Systems, *Phys. Rev. Lett.* **103**, 034102 (2009).
- [15] F. Faure and B. Zhilinskii, Topological Chern Indices in Molecular Spectra, *Phys. Rev. Lett.* **85**, 960 (2000).
- [16] V. I. Arnol'd, S. M. Goussein-Zade, and A. N. Varchenko, *Singularities of Differentiable Mappings* (Birkhauser, Boston, 1988).
- [17] H. Zoladek, *The Monodromy Group* (Birkhauser, Boston, 2006).
- [18] M. Audin, Hamiltonian monodromy via Picard-Lefschetz theory, *Commun. Math. Phys.* **229**, 459 (2002).
- [19] F. Beukers and R. H. Cushman, The complex geometry of the spherical pendulum, *Contemp. Math.* **292**, 47 (2002).
- [20] D. Sugny, P. Mardešić, M. Pelletier, A. Jebrane, and H. R. Jauslin, Fractional Hamiltonian monodromy from a Gauss–Manin monodromy, *J. Math. Phys. (N.Y.)* **49**, 042701 (2008).
- [21] See Supplemental Material at <http://link.aps.org/supplemental/10.1103/PhysRevLett.125.064301> for technical and mathematical details about Tennis Racket effect.
- [22] C. P. Koch, M. Lemesko, and D. Sugny, Quantum control of molecular rotation, *Rev. Mod. Phys.* **91**, 035005 (2019).
- [23] K. Hamraoui, L. Van Damme, P. Mardesic, and D. Sugny, Classical and quantum rotation numbers of asymmetric-top molecules, *Phys. Rev. A* **97**, 032118 (2018).
- [24] S. J. Glaser *et al.*, Training Schrödinger's cat: Quantum optimal control, *Eur. Phys. J. D* **69**, 279 (2015).
- [25] L. Van Damme, D. Leiner, P. Mardešić, S. J. Glaser, and D. Sugny, Linking the rotation of a rigid body to the Schrödinger equation: The quantum tennis racket effect and beyond, *Sci. Rep.* **7**, 3998 (2017).